Published in Proceedings of the I MECH E Part G Journal of Aerospace Engineering 2000 Vol 214 No 5 P 295-312
Archived in Dspace@NITR
http://dspace.nitrkl.ac.in/dspace
sksahu@nitrkl.ac.in

Dynamic instability of laminated composite rectangular plates subjected to non-uniform harmonic in-plane edge loading

S. K. Sahu P. K. Datta *

Department of Aerospace Engineering, I.I.T., Kharagpur, India

The dynamic instability behaviour of isotropic, cross-ply and angle-ply laminated composite plates under combined uniaxial and harmonically varying in-plane point or patch loads is investigated using finite element analysis. The first order shear deformation theory is used to model the composite laminates, considering the effects of transverse shear deformation and rotary inertia. The effect of various geometrical parameters, boundary conditions, lamination and load parameters on the principal dynamic instability regions of composite plates are studied in detail. The preferential orientations depending on the instability regions for simply-supported patch and point loaded plates have been suggested for angle ply plates. The dynamic instability regions has been influenced by the restraint provided at the edges.

Keywords: rectangular plates, composite, dynamic instability, finite element method

*Author to whom correspondence and proofs should be sent

NOTATION

a, b	Dimensions of plate
c	load band width of patch load/position of point loading
E_{11}, E_{22}	Young's modulus
G_{12}, G_{13}, G_{23}	shear modulus
$[K]$	Stiffness matrix
$[K_\sigma]$	Geometric stiffness matrix
$[M]$	Mass matrix
N_{cr}	Critical buckling load
w	Deflection of mid-plane of plate
ν_{12}, ν_{21}	Poisson's ratio
θ_x, θ_y	Rotations of the normal about axes
ρ	Mass density
$\sigma_x, \sigma_y, \tau_{xy}$	Initial in-plane stresses
Ω, ω	Frequency of forcing function and transverse vibration
α, β	Static and dynamic load factors

1 INTRODUCTION

Structural elements subjected to in-plane periodic forces may lead to dynamic instability, due to certain combinations of the values of load parameters. The instability may occur below the critical load of the structure under compressive loads over a range or ranges of excitation frequencies. Several means of combating parametric resonance such as damping and vibration isolation may be inadequate and sometimes dangerous with reverse results [1]. In contrast to the principal resonance, the parametric instability may arise not merely at a single excitation frequencies and even for small excitation amplitudes. Thus the dynamic instability characteristics are of great technical importance for understanding the dynamic systems under periodic loads. An extensive bibliography of earlier works on these problems were given in review papers [1-3]. The dynamic instability characteristics of plates subjected to uniform harmonic loads were studied by Bolotin [4] using the Fourier analysis and by Hutt and Salam [5] using thin plate finite element model. The increasing use of fibre-reinforced composite materials in automotive, marine and especially aerospace structures, has resulted interest in problems involving dynamic instability of these structures. The effect of number of layers, ply lay-up, orientation and different types of materials introduce material couplings such as stretching-bending and twisting-bending couplings etc. All these factors interact in a complicated manner on the vibration frequency spectrum of the laminates affecting the dynamic instability region. The stability behaviour of laminates is essential for assessment of the structural failures and optimal design. Birman [6] studied unsymmetric laminates on the dynamic stability of rectangular plates, neglecting transverse shear deformation and rotary inertia. Srinivasan and Chellapandi [7] analyzed laminated rectangular plates under uniaxial loading by the finite strip method. The first order shear deformation theories were used for the investigation of the dynamic instability of angle ply [8] and cross ply

[9] laminates, neglecting in-plane and rotary inertia. Tylikowski [10] studied the dynamic stability of rectangular antisymetrically laminated cross-ply plates. Chen and yang [11] studied the dynamic stability of thick laminated composite plates subjected to uniform compressive stress using Galerkin's finite element. The dynamic instability of laminated plates was investigated by Cederbaum [12,13] for uniform in-plane loading, using the method of multiple scales. The instability of composite laminated plates under uniaxial in-plane loads was investigated by Moorthy, Reddy and Plaut [14] without static load component using finite element method. The dynamic instability of layered composite plates has been studied using a high order bending theory by Kwon [15]. The instability of laminated composite plates considering geometric non-linearity was also reported [16-17]. Patel *et el.* [18] studied the dynamic instability of layered anisotropic composite plates on elastic foundations. Most of the investigators studied the dynamic stability of uniformly loaded composite plates. However, the externally applied in-plane load and boundary conditions are seldom uniform in practice. The application of non-uniform loading and boundary conditions on the structural component will alter the global quantities such as frequency, buckling load and dynamic instability region (DIR). Cases of practical interests arise when the in-plane stresses are caused by point forces acting along the boundaries and may contain singularities during analysis. The static stability analysis of a isotropic flat panel, subjected to a pair of oppositely directed in-plane concentrated forces was studied by Leissa and Ayub [19-20]. Deolasi and Datta [21] presented results of dynamic stability of thin (a/h=100), square, isotropic plates for a classical simply supported boundary conditions having three degrees of freedom per node. The present paper deals with the study of dynamic stability behaviour of rectangular isotropic, quasi-isotropic, cross-ply and angle-ply plates subjected to wide ranges of combined static and harmonically varying in-plane point or patch loads.

2 THEORETICAL ANALYSIS

The problem considered here consists of rectangular plates ($a \times b$) subjected to in-plane localized compressive edge loadings as shown in Figure 1. The angle-ply plates under investigation are assumed to be of moderately thick, thus Mindlin's first order shear deformation theory is employed. An eight nodded curved isoparametric element is employed in the present analysis with five degrees of freedom $u, v, w, \theta_x, \theta_y$ per node. The displacement field assumes that mid-plane normal remains straight before and after deformation, but not normal even after deformation so that:

$$u(x, y, z) = u_0(x, y) + z\theta_y(x, y) \tag{1}$$

$$v(x, y, z) = v_0(x, y) - z\theta_x(x, y)$$

$$w(x, y, z) = w_0(x, y)$$

where, u, v, w and u_0, v_0 and w_0 are displacement components in the x, y and z directions anywhere in the plate and at mid-plane respectively. θ_x and θ_y represent rotations of the mid-plane normal about x and y axes respectively. Green -Lagrange's strain equations are used to explain the strain displacement relations. The constitutive relationships for the laminated Mindlin plate becomes

$$\begin{Bmatrix} N_i \\ M_i \\ Q_i \end{Bmatrix} = \begin{bmatrix} A_{ij} & B_{ij} & 0 \\ B_{ij} & D_{ij} & 0 \\ 0 & 0 & S_{ij} \end{bmatrix} \begin{Bmatrix} \epsilon_j \\ k_j \\ \gamma_j \end{Bmatrix} \tag{2}$$

where A_{ij}, B_{ij}, D_{ij} and S_{ij} are the usual extensional, bending-stretching, bending and transverse shear stiffnesses. A shear correction factor of 5/6 is included in S_{ij} for all numerical computations.

2.1 Governing equations

The equation of equilibrium for free vibration of a structure subjected to periodic loads can be expressed in the form

$$N^0(t) = N_s + N_t cos\Omega t \tag{3}$$

where N_s is the static portion of load $N^0(t)$. N_t is the amplitude and Ω is the frequency of the dynamic portion of $N^0(t)$. The stress distribution in the plate will be non-uniform and periodic . Taking

$$N_s = \alpha N_{cr}, \qquad\qquad N_t = \beta N_{cr} \tag{4}$$

where α and β are the percentages of the static buckling load N_{cr}. α and β are termed as static and dynamic load factors respectively. In this analysis, the buckling load for a fully loaded plate is taken as the reference load. Using Eq. (4), the equation of motion in matrix form is obtained as:

$$[M]\{\ddot{q}\} + [[K_e] - \alpha N_{cr}[K_g] - \beta N_{cr}[K_g] cos\Omega t]\{q\} = 0 \tag{5}$$

Eq. (5) represents a system of second order differential equations with periodic coefficients of the Mathieu-Hill type. The development of regions of instability arises from Floquet's theory which establishes the existence of periodic solutions. The boundaries of the dynamic instability regions are formed by the periodic solutions of period T and 2T, where $T = 2\pi/\Omega$. The boundaries of the primary instability regions with period 2T are of practical importance [4] and the solution can be achieved in the form of the trigonometric series

$$q(t) = \sum_{k=1,3,5}^{\infty} \left[\{a_k\} sin\frac{k\theta t}{2} + \{b_k\} cos\frac{k\theta t}{2} \right] \tag{6}$$

Putting this in Eq.(5) and if only first term of the series is considered, equating coefficients of $sin\frac{\theta t}{2}$ and $cos\frac{\theta t}{2}$, the equation (5) reduces to

$$\left[[K_e] - \alpha N_{cr}[K_g] \pm \frac{1}{2}\beta N_{cr}[K_g] - \frac{\Omega^2}{4}[M] \right] \{q\} = 0 \tag{7}$$

Eq. (7) represents an eigenvalue problem for known values of α, β and N_{cr}. The two conditions under a plus and minus sign correspond to two boundaries of the dynamic instability region (DIR). The eigenvalues are Ω, which give the boundary frequencies of the instability regions for given values of α and β.

The element matrices can be expressed as:

Elastic stiffness matrix

$$[K_e]_e = \int [B]^T [D][B] dxdy \tag{8}$$

Geometric stiffness matrix

$$[K_\sigma]_e = \int [B_g]^T [\bar{\sigma}][B_g] dxdy \tag{9}$$

Consistent mass matrix

$$[M]_e = \int [N]^T [I][N] dxdy \tag{10}$$

The overall matrices $[K_e], [K_\sigma]$ and [M] are obtained by assembling the corresponding element matrices. The vector of generalized coordinates consists of only active nodal displacements.

2.2 Computer program

A program has been developed to perform all the necessary computations. The element stiffness and mass matrices are derived using a standard procedure. The geometric stiffness matrix is essentially a function of the in-plane stress distribution in the element due to applied edge loading. Since the stress field is non-uniform, plane stress analysis is carried out using the finite element techniques to determine the stresses and these stresses are used to formulate the geometric stiffness matrix. Reduced integration technique is adopted for the element matrices in order to avoid possible shear locking. The overall matrices $[K_e], [K_\sigma]$ and [M] are obtained by assembling the corresponding element matrices, using skyline technique. Subspace iteration method is adopted throughout to solve the eigenvalue problems.

3 RESULTS AND DISCUSSION

Numerical results are presented for rectangular isotropic and laminated composite plates with different combinations of boundary conditions. S and C denote a simply-supported and clamped edge respectively. The notation SCSC identifies a plate with the edges simply supported at x=0, a and clamped at y=0, b. The following boundary conditions for simply supported (S), clamped (C) are assumed for the first order shear deformation theory:

Isotropic/ quasi-isotropic/ cross-ply

S: v=w=θ_x=0 at x=0, a and u=w=θ_y=0 at y=0, b

C: u=v=w=$\theta_x = \theta_y$=0 at any edge

Angle-ply

S: u=w=θ_x=0 at x=0, a and v=w=θ_y=0 at y=0, b

C: u=v=w=$\theta_x = \theta_y$=0 at any edge.

3.1 Convergence study

The convergence studies have been carried out for free vibration for a composite plate in Table 1 and compared with the results of Bert and Chen [22]. The convergence study on buckling due to a pair of concentrated load is studied for a isotropic plate in Table 2 and the results are compared with Leissa and Ayub [19]. The study shows good convergence of the numerical solutions. A 10×10 mesh has been employed to idealize the flat panel in the subsequent analysis. This idealisation is chosen in order to apply compression to a small fraction of the edge length and also for convergence criterion.

The present formulation is then validated for free vibration analysis of angle-ply and cross ply plates. The results are presented in Tables 3 and 4, showing good comparison with the literature. To validate the formulation further, the buckling results for angle-ply and cross ply plates are shown in Tables 5 and 6 respectively and compared with those available in

the literature. The above studies indicate good agreement exits between the present study and those from the literature. Once the free vibration and buckling results are validated, the dynamic instability studies are made.

3.2 Dynamic instability studies

The dynamic instability studies are made for isotropic, quasi-isotropic, cross-ply and angle-ply plates with a moderately thick plate (b/h=25), subjected to patch and point in-plane loading throughout the investigation. A 'standard case' is defined for the problem in which, the geometrical and material properties are as follows [14]:

a=250 mm, b=250 mm, h=10 mm,

$E_1/E_2 = 40, G_{12}/E_2 = G_{13}/E_2 = 0.6, G_{23}/E_2 = 0.5, \nu = 0.25.$

The computed fundamental frequency of vibration (ω), and first critical buckling load (N_{cr}) are considered for the determination of stability regions. Dynamic instability regions (DIR) are plotted in the plane having load frequency (Ω/ω) as abscissa and load amplitude ($\beta = N_t/N_{cr}$) as ordinate. The instability mode shapes for a laminate under patch load and point loads are shown in Figure 2.

3.2.1 Isotropic plate

The instability regions are plotted for patch loading from one end to study the effect of load band width and compared with Ref [21]. The study shows good agreement with the results as given in Figure 3. The instability studies are then extended to study the effect of static load factor, aspect ratio and boundary conditions of a moderately thick plate. The effect of static load factor on instability of partially loaded thick plate is shown in Figure 4. It is observed that with the increase of static load factor from 0.2 to 0.6, the onset of dynamic stability occurs earlier and the width of dynamic instability region (DIR) also increases. The effect of aspect ratio (a/b=1, 2, 3) on the DIR is shown in Figure 5. The

study reveals that the onset of instability occurs earlier for rectangular plates than square plate. However, the width of DIR is narrower for rectangular plates in comparison with square plates. The effect of boundary conditions on dynamic instability regions is shown in Figure 6. As expected, the onset of instability occurs later and also the width of DIR is smaller with increase of restraint at the edges. The study is further carried out for laminated composite cross-ply and angle-ply plates. The instability studies for c/b=1 correspond to the plate under uniaxial, uniform harmonic loading for which references are available [7-14]. The investigation is then extended for patch and point edge loads. The parametric studies at c/b=0 correspond to point harmonic loads at the two opposite edges. To validate the formulation, the principal instability regions for uniform loading are plotted and compared.

3.2.2 Cross ply plate

The instability results of a cross ply plate with ply lay-up 0/90/90/0 is taken as a standard case and compared with the literature. The study shows good agreement with results of Moorthy *et al.* [14]. Then the study is extended to the instability criteria of a quasi-isotropic material with ply lay-up 0/-45/45/90 [27] and compared in Figure 7. The onset of dynamic instability occurs earlier for quasi-isotropic plates with wider instability regions. The effect of aspect ratio on dynamic instability regions of cross ply plates is shown in Figure 8. As in isotropic plates, the onset of instability occurs later for square plates but with wider instability zones.

3.2.2.1 Non uniform loading

The instability behaviour of cross ply plates subjected to various non-uniform harmonic loads including patch and point loads is studied. The effect of load band width on instability behaviour under patch loading (load case (a) and (b) in Figure 1) is shown in Figure 9. It is observed that for small values of c/b (=0.2), the onset of instability occurs later with narrow

width of dynamic instability region in comparison with higher load band width. This may be due to restraint of the edge, which has a stabilizing effect on the instability behaviour for a small load band width. As observed from Figure 9, the onset of instability occurs earlier with wide DIR for load case (b) than that of load case (a). The effect of positions of point loads on the instability of cross ply plates is also studied. As shown in Figure 10, the onset of instability occurs later for the load near the edges with narrow DIR. This indicates that the structure is more stable for point loads near the edges.

3.2.3 Angle-ply plate

The numerical results have been presented with non-dimensionalisation parameter relative to ω and N_{cr} of the four layer $(\pm 45^0)_2$ anti-symmetric angle-ply plate. To validate the formulation, the principal instability regions for uniform loading are plotted and compared.

3.2.3.1 Uniform loading

The parametric instability regions are plotted for a uniformly loaded anti-symmetric angle-ply plate without static component to consider the effect of number of layers. It is observed from Figure 11 that the structure is more stable under periodic loads with increase of number of layers showing instability regions at higher frequencies and narrower, which compares well with the literature [14]. The observed behaviour is attributed to the effect of bending-stretching coupling for the case of laminates, due to decrease of effective stiffness. Then the effect of ply orientation is also studied for four and two layer laminates as shown in Figure 12. The effect of ply orientation is symmetrical with respect to 45^0. It is observed from Figure 12 (a) that the greater the ply orientation the smaller the instability region for four layer laminate. The above studies indicate good agreement between the present study and the literature. In the case of two layer angle-ply laminate (Figure 12 (b), the effect of ply orientation is symmetrical but the preferential orientation is now 0^0 but not 45^0. This

is may be due to the dominance effect of bending-stretching coupling for 0^0 ply orientation. Similar conclusions are also obtained for the effect of ply orientation on free vibration of anti-symmetric angle-ply laminate by Jones [27]. The effect of bending-stretching coupling found to be significantly reduced with four layer laminate and all further parametric studies are done with a four layer laminate combination. The effect of static component of load for α=0.0, 0.2, 0.4, 0.6 and 0.8 on the instability region is shown in Figure 13. Due to increase of static component, the instability regions tend to shift to lower frequencies and become wider. All further studies are made with a static load factor of 0.2 (unless otherwise mentioned). The effect of aspect ratio is studied for a/b=1, 2 and 3. As shown in Figure 14, the onset of instability occurs later for square plates than rectangular plates but with wider instability region, similar to isotropic and cross ply laminates. Figure 15 shows the effect of thickness on the instability region. It is observed that onset of instability occurs later with narrow instability regions showing more stiffness, with increase of thickness of a laminate. Then the study is extended to instability of angle-ply plates subjected to various non-uniform harmonic loading.

3.2.3.2 Non-uniform loading

Figure 16 shows the instability regions for the load case (a) in Figure 1 for $c/b = 0.2$ and $c/b = 0.8$ for different orientations. Here the effect of ply orientation is not symmetrical with respect to 45^0 as in uniform loading. It appears from Figure 16(a) that the instability regions of plates having $0^0, 15^0$and 30^0 ply orientations are narrow in comparison with other ply orientations. Plates with 30^0 orientation shows instability at higher frequencies reflecting it to be stiffer. Plates with ply-ups of $60^0, 75^0$ and 90^0 show wider instability regions for this loading with smaller frequencies. But the patch loaded plates for $c/a = 0.8$ show narrow instability regions at 30^0 and 45^0. The plates with 45^0 ply-orientations seem to be

stiffer due to shifting to higher frequencies. As expected, the plates with $75^0, 90^0$ lay-ups show instability at lower frequencies with wide instability regions. As the load band width increases from 0.2 to 0.8 (Figure 16(b)), the onset of instability frequencies shift towards to that of a uniformly loaded plate. But in the case of load case (b), which is more general than load case (a), the trends are more clear (Figure 17). It is observed from Figure 17(a) that the ply-orientation of 30^0 for $c/b = 0.2$ seems to be the most stiff in consideration of higher frequency and width of instability region. However, the plates with 45^0 orientation show maximum stiffness and narrow instability region at $c/b = 0.8$ as shown in Figure 17(b). The instability regions for the point loads are shown in Figure 18. Figure 18 (a) indicates narrow instability zones for ply orientations of $0^0, 15^0$ and 30^0 for load case (c) of Figure 1. This also shows wide zones of instability for $60^0, 75^0, 90^0$ lay-ups. However, the plates of $(\pm 30^0)_2$ orientation shows more stiffness due to shifting to higher frequencies. The results of the instability regions for load case (d) for different orientations are shown in Figure 18(b). The results also indicate that the $0^0, 15^0$ and 30^0 have narrow instability regions in comparison with other lay-ups.

4 CONCLUSION

The results from a study of the instability behaviour of isotropic, quasi-isotropic, cross-ply and anti-symmetric angle-ply plates subjected to uniform and non-uniform periodic in-plane edge loading can be summarized as follows.

1. The onset of instability occurs earlier for rectangular than square plates but with wider instability regions.

2. Due to static component, the instability regions tend to shift to lower frequencies showing destabilizing effect on the dynamic stability behaviour of the plate.

3. The onset of instability occurs later with narrow zones of instability with addition of restraint at the edges.

4. The instability occurs earlier for quasi-isotropic plates than laminated plates.

5. The laminated composite plates become more stiff with more number of layers.

6. The effect of ply orientation is symmetric. 0^0 and 45^0 seems to be the preferential orientations for uniformly loaded 2 and 4 layer anti-symmetric angle-ply plates respectively.

7. The onset of instability occurs later with narrow instability regions showing more stiffness, with increase of thickness of a laminate.

8. Dynamic instability behaviour under patch compression loading shows that the width of the instability region increases as the load band width increases.

9.The partial loaded angle-ply plates behave differently to that of uniformly loaded plate. $(\pm 30^0)_2$ seems to be the preferential orientation angle for design consideration of instability for a small load band width. As the load band width increases gradually the frequencies shift towards a uniformly loaded plate with a optimum ply orientation at 45^0.

10. However the plates of $(\pm 30^0)_2$ orientation shows more stiffness due to shifting to higher frequencies and seems to be the preferential orientation for concentrated loaded plates.

REFERENCES

1. Evan-iwanowski, R. M. On the parametric response of structures. *Appl. Mechanics Review*, 1965, **18**, 699-702 .

2. Ibrahim, R. A. Parametric Vibration Part III. Current problems (1).*Shock and Vibr. Digest*, 1978, **10**, 41-57.

3. Simitses, G. J. Instability of dynamically loaded structures. *Appl. Mechanics Review*, 1987, 40, 1403-1408.

4. Bolotin, V. V. *The Dynamic Stability of Elastic System*, 1964, Holden-Day, San Francisco.

5. Hutt, J. M. and Salam, A. E. Dynamic stability of plates by finite elements, *J. Engrg. Mechanics Division, ASCE*, 1971, **EM 3**, 879-899.

6. Birman, V. Dynamic stability of unsymmetrically laminated rectangular plates. *Mech. Res. Commun.*, 1985, **12**, 81-86

7. Srinivasan, R. S. and Chellapandi, P. Dynamic stability of rectangular laminated composite plates, *Comput. Struct.*, 1986, **24**(2), 233-238.

8. Bert, C. W. and Birman, V. Dynamic instability of shear deformable antisymmetric angle-ply plates. *Int. J. Solids Structs.*, 1987, **23**(7), 1053-1061.

9. Librescu, L. and Thangjitham, S. Parametric instability of laminated composite shear deformable flat panels subjected to in-plane edge loads, *Int. J. Non-linear Mechanics*, 1990, **25**, (2,3), 263-273.

10. Tylikoski, A. Dynamic stability of nonlinear antisymmetrically laminated cross-ply rectangular plates, *ASME J. Appl. Mechanics*, 1989, **56**, 375-381.

11. Chen, L. W. and Yang, J. Y. Dynamic stability of laminated composite plates by the finite element method,*Comput. Struct.*,1990, **36**(5),845-851.

12. Mond, M. and Cederbaum, G. Dynamic instability of antisymmetric laminated plates, *J. Sound Vibr.*, 1992, **154**, (2), 271-279.

13. Cederbaum, G. Dynamic stability of shear deformable laminated plates, *AIAA Journal*, 1991, **29**, 2000-2005.

14. Moorthy, J. Reddy, J. N. and Plaut, R. H. Parametric instability of laminated composite plates with transverse shear deformation, 1990, *Int. J. Solids Structs.*,**26**(7), 801-811.

15. Kwon, Y.W. Finite element analysis of dynamic instability of layered composite plates using a high order bending theory. *Comput. Struct.*, 1991, **38**(1), 57-62.

16. Balamurugan, V. , Ganapathi, M. and Varadan, T. K. Nonlinear dynamic stability of laminated composite plates using finite element method. *Comput. Struct.*, 1996, **60**, (1), 125-130.

17. Ganapathi, M. , Boisse, P. and Solaut, D. Nonlinear dynamic stability analysis of composite laminates under periodic in-plane compressive loads. *Int. J. Num. Meth. Engrg.*, 1999, **46**, 943-956.

18. Patel, B. P. , Ganapathi, M. , Prasad, K. R. and Balamurugan, V. Dynamic instability of layered anisotropic composite plates on elastic foundations, *Engrg. Structs.*, 1999, **21**, 988-995.

19. Leissa A. W. and E. F. Ayub. Vibration and buckling of simply supported rectangular plate subjected to a pair of in-plane concentrated forces. *J. Sound Vibr.*,1988, **127**, 155-171

20. Leissa A. W. and E. F. Ayub. Tension buckling of Rectangular sheets due to concentrated forces," *J. Engrg. Mechanics, ASCE*, 1989, **115**, 2749-2762

21. Deolasi, P. J. and Datta, P. K. Parametric instability characteristics of rectangular

plates subjected to localized edge loading (compression or tension). *Comput. Struct.*, 1995, **54**(1), 73-82.

22. Bert, C. W. and Chen, T. L. C. Effect of shear deformation on vibration of anti-symmetric angle ply laminated rectangular plates.*Int. J. Solids Structs*, 1978, **14**, 465-473.

23. Reddy, J. N. and Phan, N. D. Stability and vibration of isotropic, orthotropic and laminated plates according to a higher-order shear deformation theory. *J. Sound Vibr.*, 1985,**98**(2), 157-170.

24. Khdeir, A.A. and Reddy, J.N. Free vibrations of laminated composite plates using second order shear deformation theory.,*Comput. Struct.*, 1999,**71**, 617-626.

25. Narita, Y. and Leissa, A.W. Buckling studies for simply supported symmetrically laminated rectangular plates. *Int. J. Mech. Sci*, 1990, **32**, 909-924.

26. Nair, S., Singh. G. and Rao, G.V. Stability of laminated composite plates subjected to various types of in-plane loadings. *Int. J. Mech. Sci.*, 1996, **38**, 191-202.

27. Jones, R.M. *Mechanics of Composite Materials*, 1975, McGraw-Hill book Company.

Table 1 Convergence of non-dimensional free vibration frequencies of four layer anti-symmetric angle-ply square plates for different ply orientations.

$$a/b = 1, a/h = 10, E_{11}/E_{22} = 40, G_{23} = 0.5E_{22}, G_{12} = G_{13} = 0.6E_{22}, \nu_{12} = 0.25$$

Non dimensional frequency, $\bar{\omega} = \omega a^2 \sqrt{(\frac{\rho}{E_{22}h^2})}$

Mesh	Non-dimensional frequencies for different ply orientation			
Division	(5/-5/5/-5)	(15/-15/15/-15)	(30/-30/30/-30)	(45/-45/45/-45)
4×4	14.7545	15.6192	17.6471	18.4747
8×8	14.7428	15.6066	17.6331	18.4601
10×10	14.7424	15.6061	17.6325	18.4596
	(14.74)	(15.61)	(17.63)	(18.46)

The values given within parenthesis are from Ref. [22].

Table 2 Convergence of non-dimensional buckling loads for simply-supported rectangular plates under point loading for different aspect ratio and position of load.

Non dimensional buckling load, $\lambda = N_x b^2/D, D = \frac{Eh^3}{12(1-\nu^2)}$

a/b	c/b	N on-dimensional buckling load			
		Present FEM			Ref [19]
		4×4	8×8	10×10	
1	0.5	25.8981	25.6446	25.6478	25.814
	0.25	37.6665	36.2720	36.3069	37.000
2	0.5	42.0364	28.7918	28.6564	28.523
	0.25	50.8079	36.8657	36.6842	36.954

Table 3 Non-dimensional free vibration frequencies of multi-layered simply-supported anti-symmetric angle-ply laminated square plate .

$$E_{11}/E_{22} = 40, G_{23} = 0.5E_{22}, G_{12} = G_{13} = 0.6E_{22}, \nu_{12} = 0.25$$

Non dimensional frequency, $\bar{\omega} = \omega a^2 \sqrt{(\frac{\rho}{E_{22}h^2})}$

a/h	45/-45			45/-45/45/-45			45/-45..(8 layers)		
	Present	Ref [11]	Ref [23]	Present	Ref [11]	Ref [23]	Present	Ref [11]	Ref [23]
5	10.333	10.335	10.35	12.627	-	12.64	12.889	12.892	12.90
10	10.042	10.044	10.35	18.4596	18.46	18.49	19.285	19.289	19.31
20	14.179	14.179	14.22	21.870	21.87	21.92	23.257	23.259	23.31
25	14.338	14.338	-	22.4248	-	-	23.923	23.924	-
50	14.561	14.561	14.66	23.237	23.24	23.32	24.909	24.909	25.00
100	14.618	14.618	14.90	23.455	-	23.66	25.176	25.176	25.38

Table 4 Non-dimensional free vibration frequencies of a two-layer anti-symmetric cross-ply laminated square plates (0/90).

$$E_{11}/E_{22} = 25, G_{23} = 0.2E_{22}, G_{12} = G_{13} = 0.5E_{22}, \nu_{12} = 0.25$$

Non dimensional frequency, $\bar{\omega} = \omega a^2\sqrt{(\frac{\rho}{E_{22}h^2})}$

Boundary	Non-dimensional frequencies			
condition	a/h=5	a/h=10	a/h=20	a/h=50
SSSS	7.3901	8.9003	9.4750	9.6600
	(7.609)	(8.900)	(9.504)	(9.665)
SCSS	8.1295	10.6120	11.8054	12.2358
	(8.454)	(10.803)	(11.872)	(12.247)
SCSC	8.9334	12.6225	14.8748	15.8097
	(9.377)	(12.622)	(15.015)	(15.835)

The values given within parenthesis are from Ref [24]

Table 5 Comparison of buckling loads for thin simply-supported uniformly loaded angle-ply $(\theta^0/-\theta^0/\theta^0)$ plates.

$$E_{11} = 60.7, E_{22} = 24.8, G_{12} = 12.0, \nu_{12} = 0.23, a/h = 100$$

$$\lambda = N_x b^2/D_o,\ D_o = E_{11}h^3/12(1-\nu_{12}\nu_{21})$$

Angle in	Non-dimensional buckling loads		
degree	Present FEM	Ref[25]	Ref[26]
0	23.3766	23.39	23.3778
15	24.0053	24.04	23.9906
30	25.3313	25.42	25.2778
45	26.0241	26.14	25.9514
60	25.3332	25.42	25.2778
75	24.0074	24.04	23.9906
90	23.3766	23.39	23.3778

Table 6 Comparison of buckling loads for simply-supported cross-ply laminated square plates

.

$$E_{11}/E_{22} = 40, G_{12} = G_{13} = 0.6E_{22}, G_{23} = 0.5E_{22}, \nu_{12} = 0.25$$

Non dimensional buckling load, $\lambda = N_x b^2/E_2 h^3$

a/h	0/90		0/90/0		0/90/90/0	
	Present FEM	Ref [23]	Present FEM	Ref [23]	Present FEM	Ref [23]
5	7.906	8.628	10.727	11.008	11.4482	11.533
10	11.1137	11.099	22.0907	22.16	23.233	23.27
20	12.4344	12.268	31.0885	30.922	31.599	31.432
25	12.6172	12.395	32.7316	32.515	33.0878	33.089
50	12.8706	12.569	35.2337	34.936	35.3344	35.1
100	12.9358	12.614	35.9242	35.602	35.9501	35.645

Illustration No 1

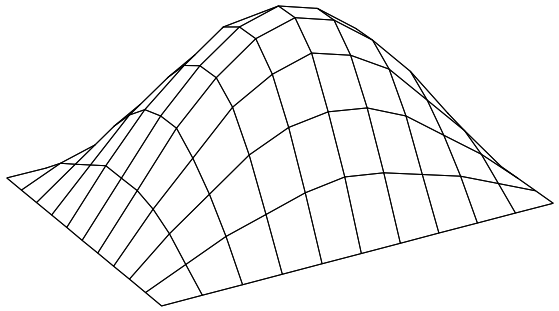

2nd frequency
patch loading, c/b=0.2, $d \overset{(a)}{=} 0.2$, b=0.4

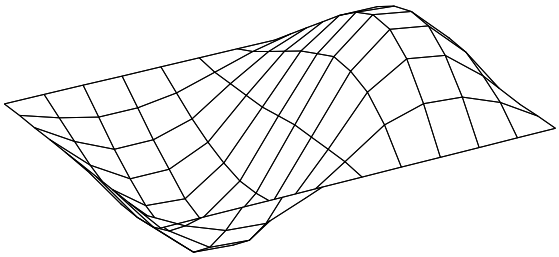

Illustration No 2

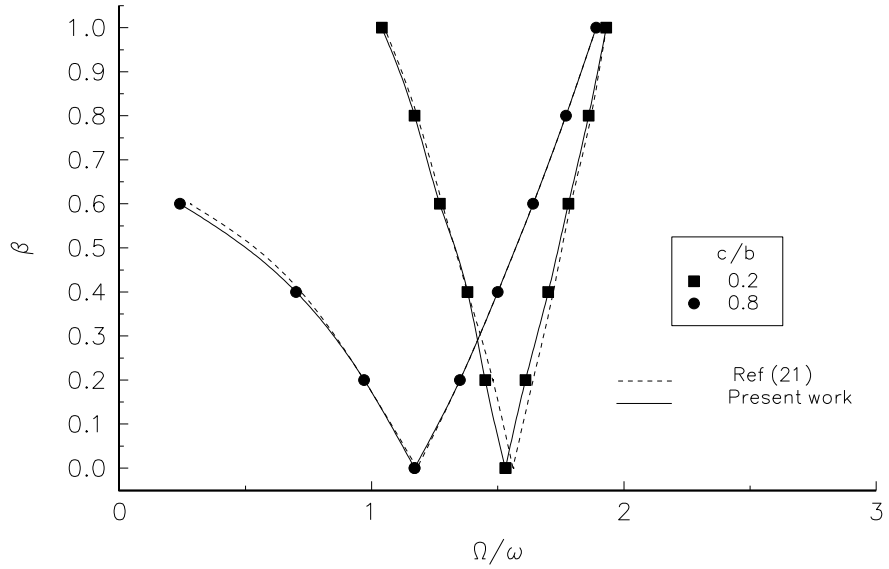

Illustration No 3

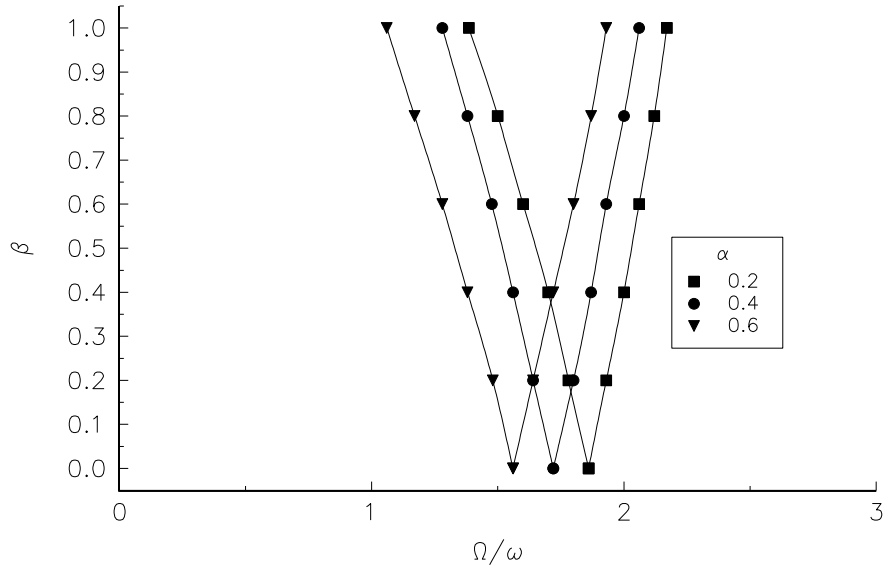

Illustration No 4

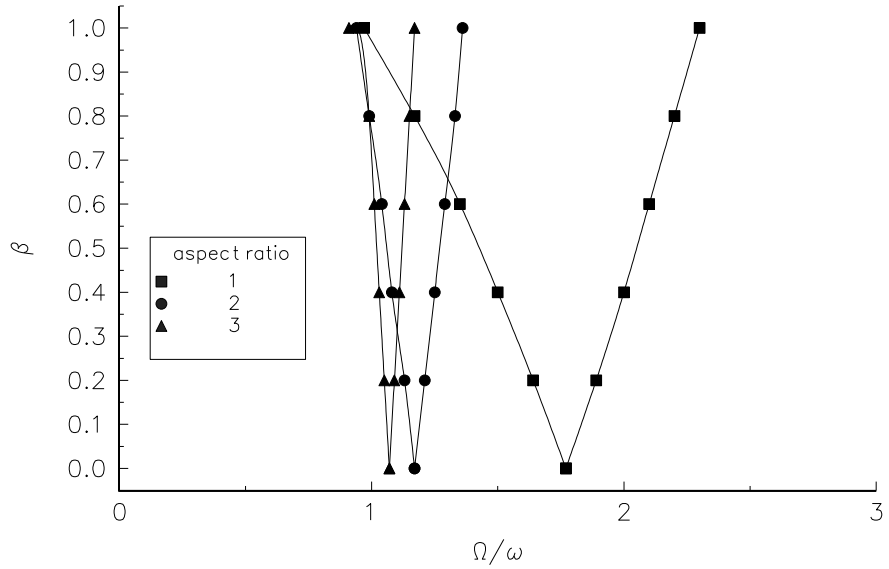

Illustration No 5

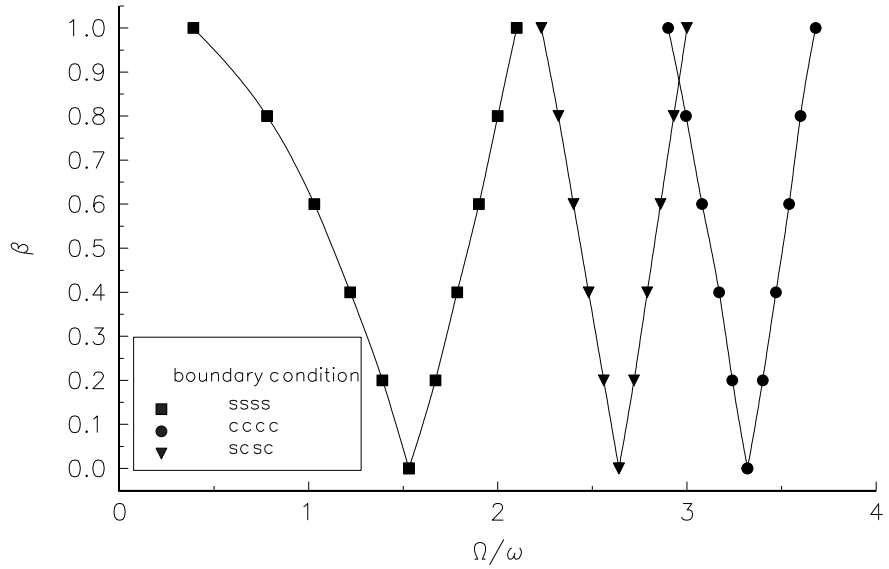

Illustration No 6

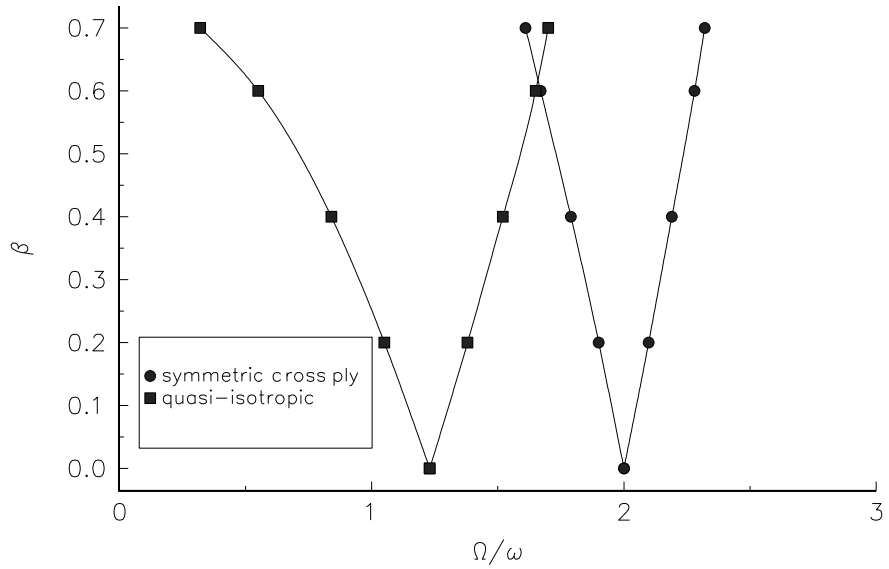

Illustration No 7

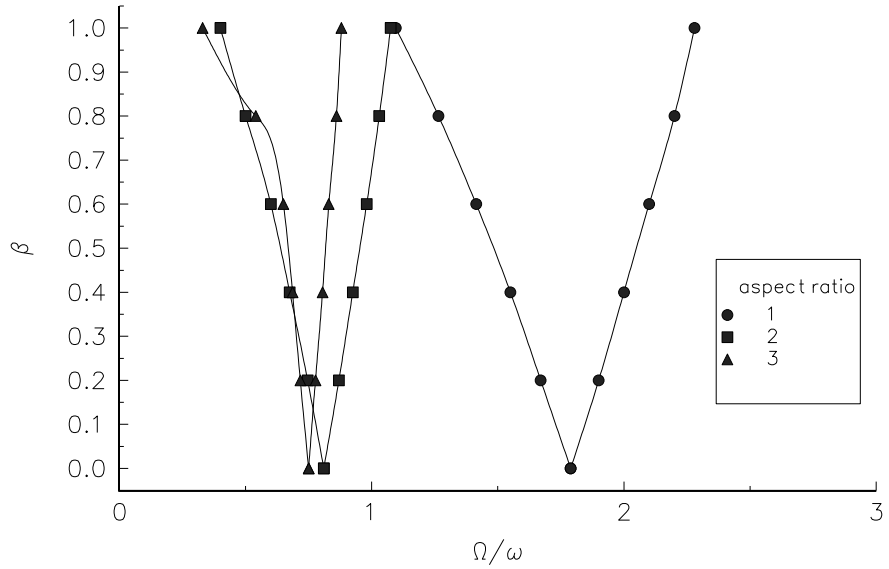

Illustration No 8

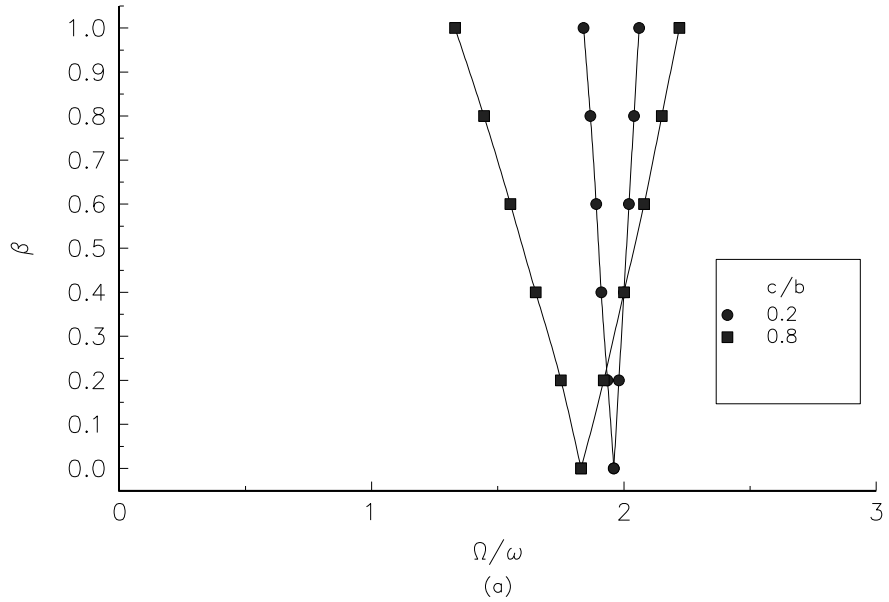

(a)

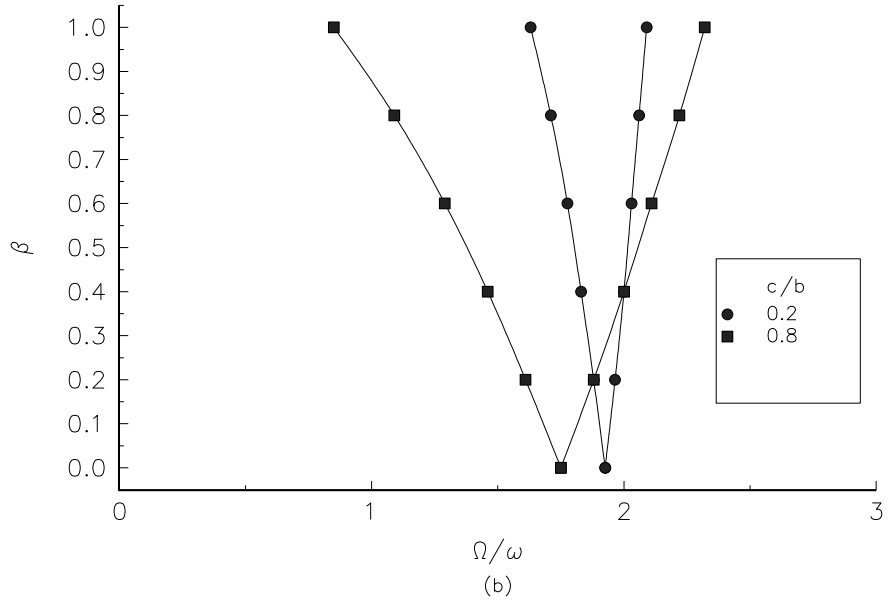

(b)

Illustration No 9

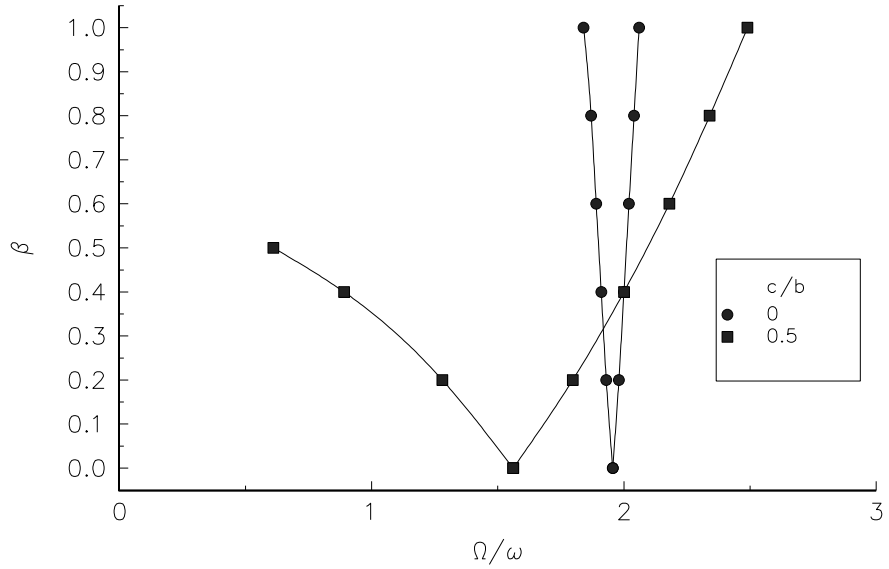

Illustration No 10

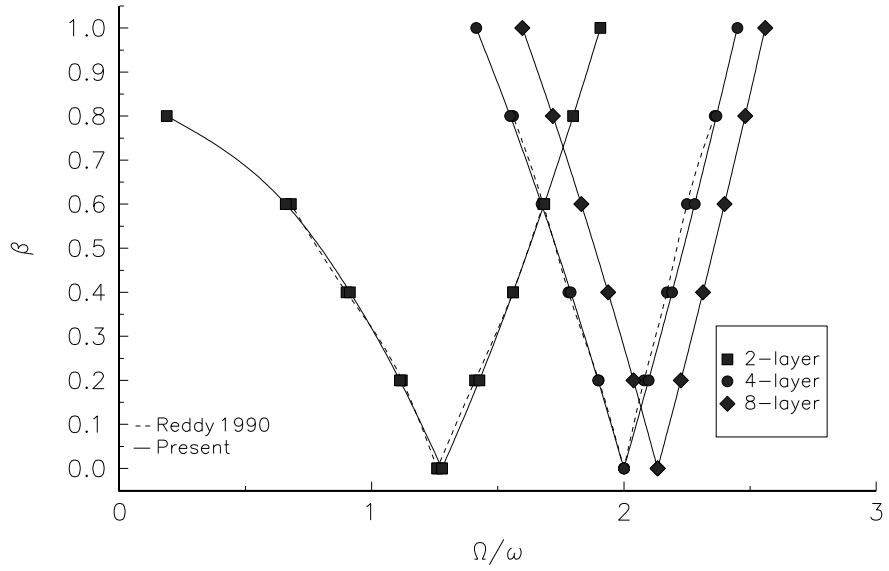

Illustration No 11

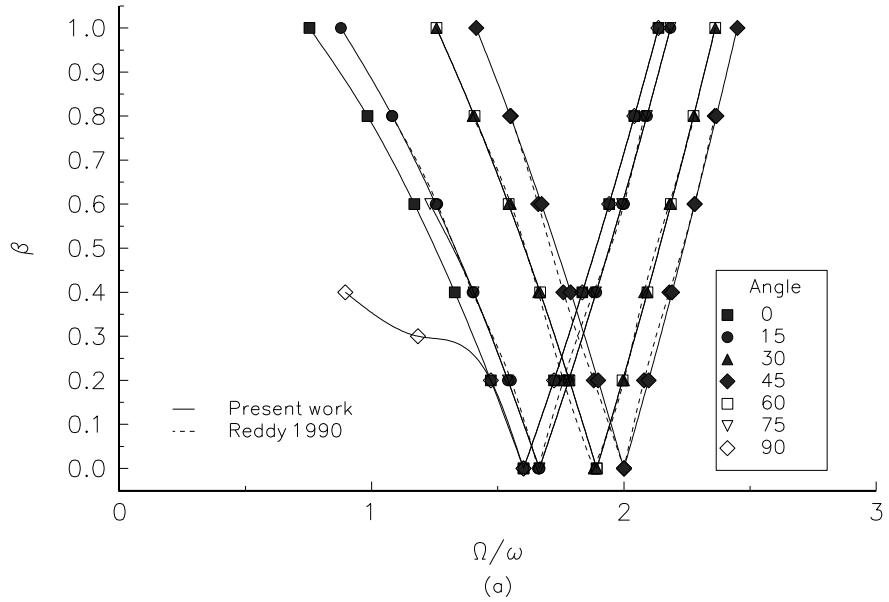

(a)

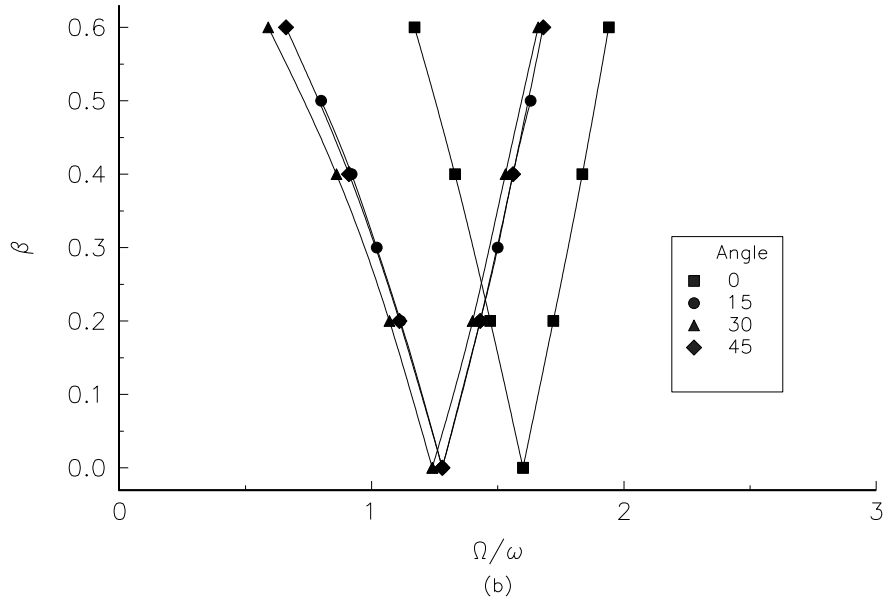

(b)

Illustration No 12

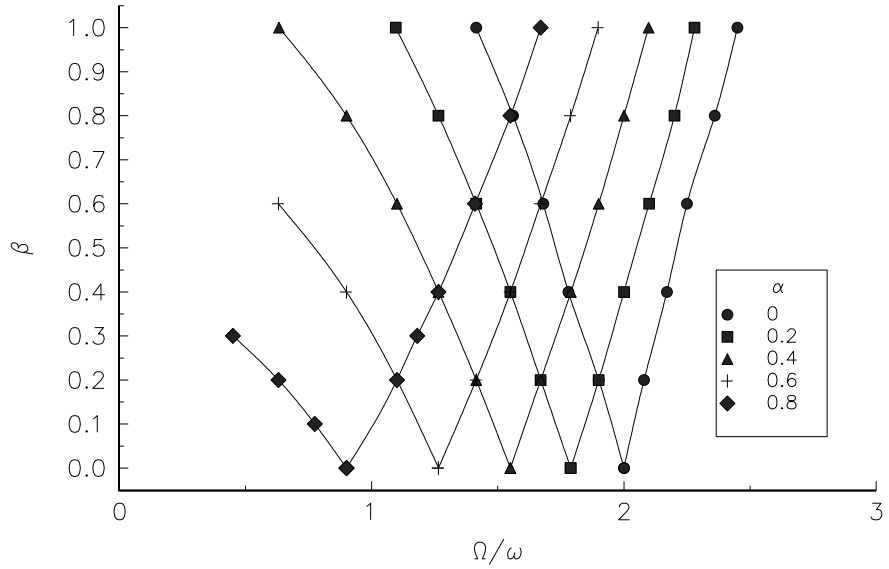

Illustration No 13

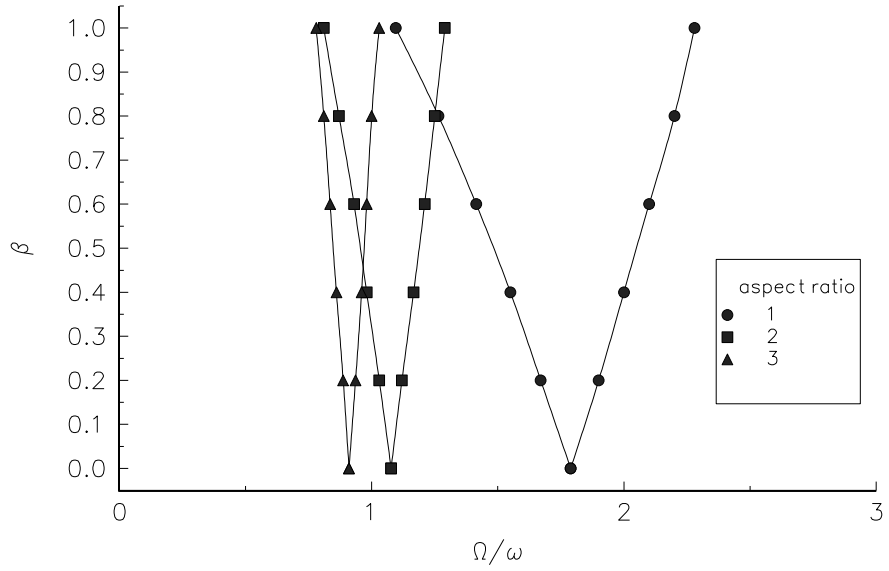

Illustration No 14

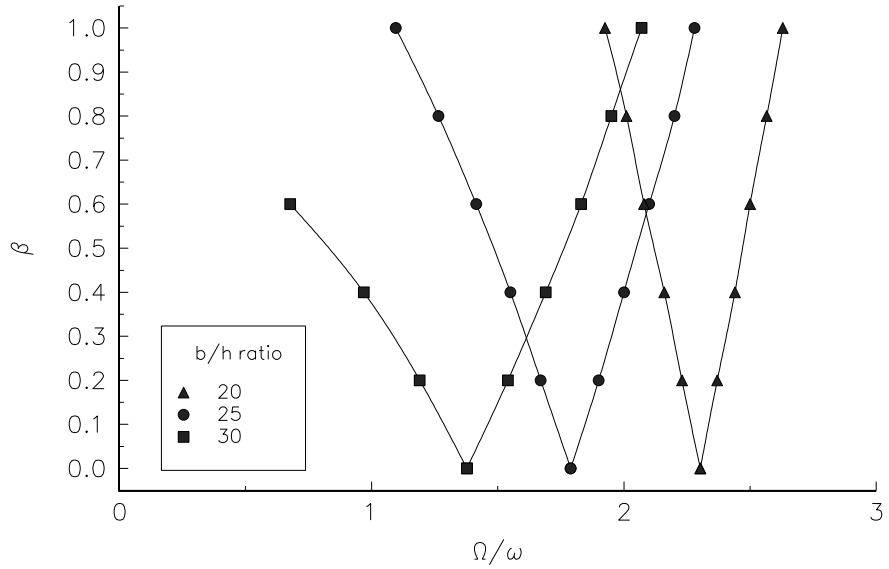

Illustration No 15

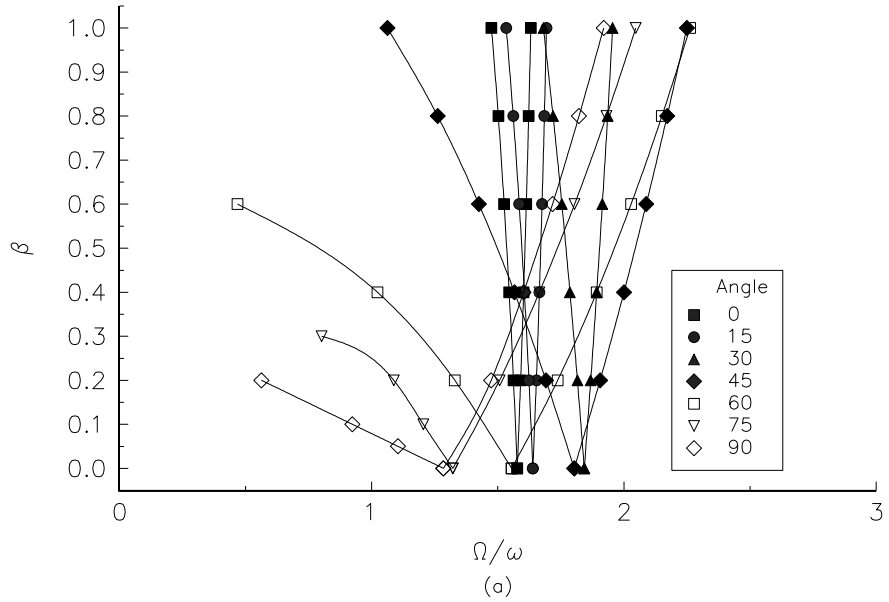

(a)

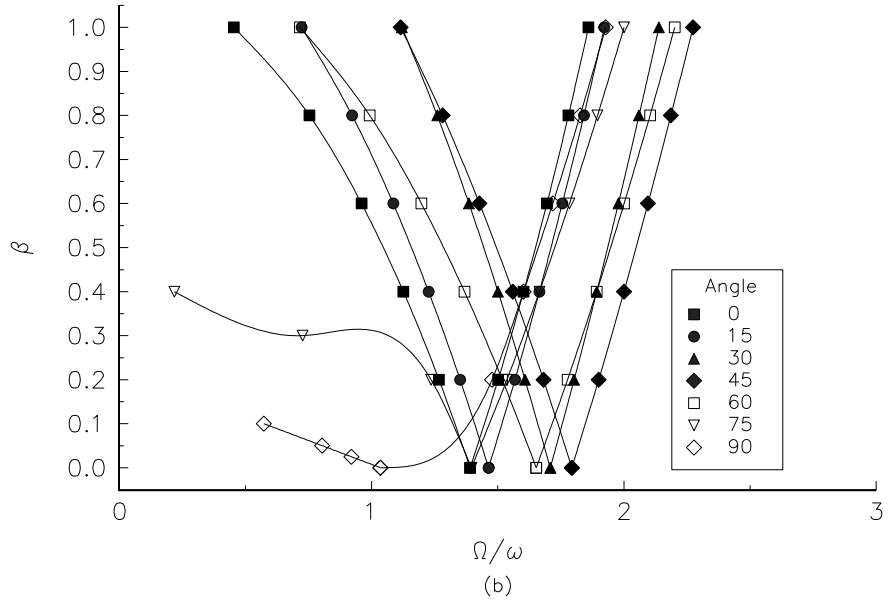

(b)

Illustration No 16

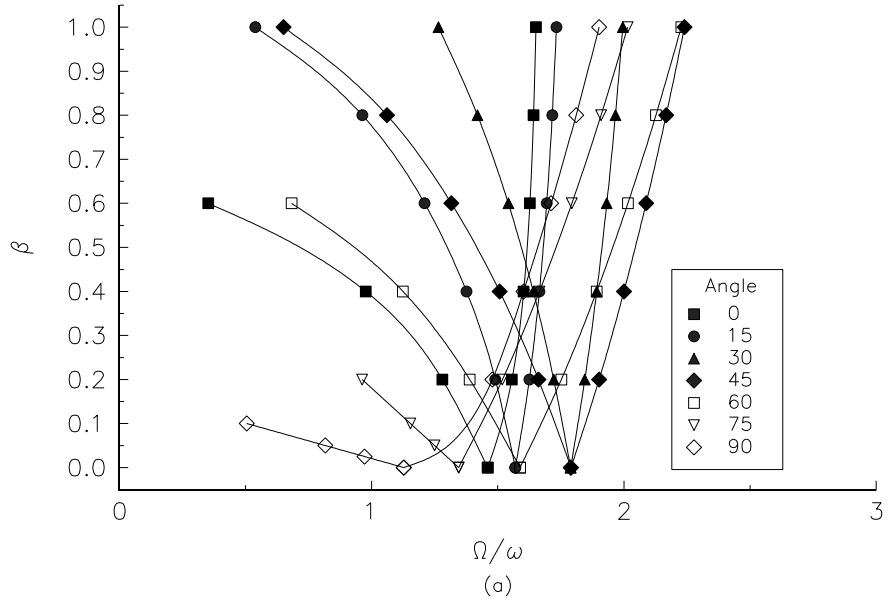

(a)

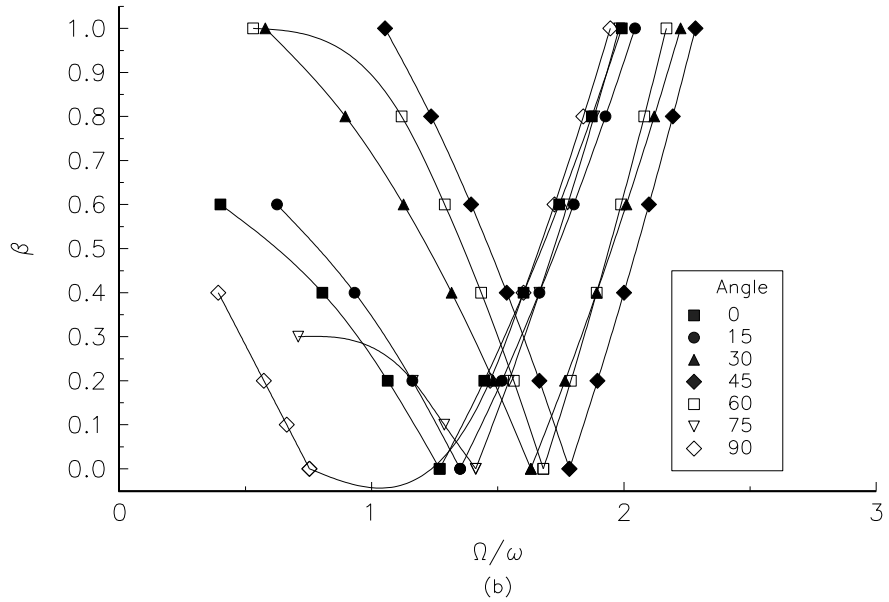

(b)

Illustration No 17

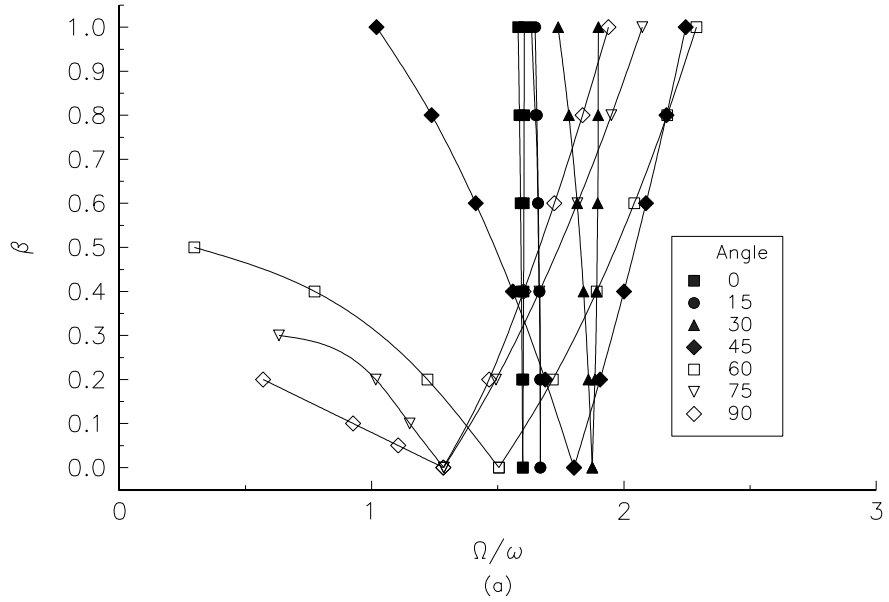

(a)

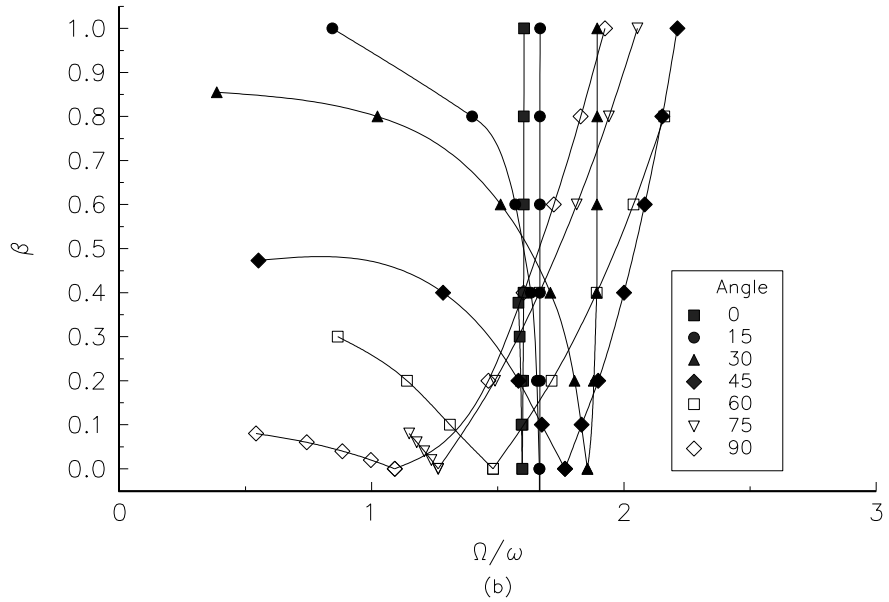

(b)

Illustration No 18

Captions to illustrations

Figure 1 Description of the plate problem: (a) partial edge loading at both ends;(b) partial edge loading at one end ; (c) pair of concentrated edge loading at both ends; (d) pair of concentrated edge loading at one end.

Figure 2 Details of instability mode shapes for angle-ply (45/-45/45/-45) plate under non-uniform loading: a) patch load from one end, c/b=0.2, α=0.2; b) point load from both ends, c/b=0, α=0.2

Figure 3 Effect of load band width on regions of dynamic instability for isotropic patch compression loading, load case 1(a), a/b=1, b/h=100, $\nu = 0.3, \alpha = 0.6$

Figure 4 Effect of static load factor on regions of dynamic instability for isotropic patch compression loading at one end, a/b=1, b/h=25, c/b=0.2, $\nu = 0.3, \alpha = 0.2, 0.4, 0.6$

Figure 5 Effect of aspect ratio on regions of dynamic instability for isotropic patch compression edge loading at one end, a/b=1, 2 and 3, b/h=25, c/b=0.8 $\nu = 0.3, \alpha = 0.2$

Figure 6 Effect of boundary condition (SSSS, SCSC, CCCC) on regions of dynamic instability for isotropic partial compression loading at one end, a/b=1, b/h=25, c/b=0.5, $\nu = 0.3, \alpha = 0.4$

Figure 7 Regions of dynamic instability for quasi-isotropic and cross-ply fully loaded compression loading at one end, a/b=1, b/h=25, $\alpha = 0.0$

Figure 8 Effect of aspect ratio on regions of dynamic instability for cross ply uniformly loaded compression at one end, a/b=1, 2 and 3,$\alpha = 0.2$

Figure 9 Effect of load band width on regions of dynamic instability for patch loaded cross-ply laminate: a) a/b=1, $\alpha = 0.2$, load case (a) ; b) a/b=1, $\alpha = 0.2$, load case (b)

Figure 10 Effect of position of loads on regions of dynamic instability for cross ply subjected

to concentrated loading, a/b=1, c/b=0.0 and 0.5, $\alpha = 0.2$

Figure 11 Effect of number of layers on instability region of a uniform loaded anti-symmetric angle-ply plate, c/b=1.0, $\alpha = 0.0$.

Figure 12 Effect of ply orientation on instability region of uniform loaded anti-symmetric angle-ply plate: a) 4 layer, c/b=1.0, $\alpha = 0.0$; b) 2 layer, c/b=1.0, $\alpha = 0.0$.

Figure 13 Effect of static load factor on instability regions of for uniform loaded anti-symmetric angle-ply plate, a/b=1, α=0.0, 0.2, 0.4, 0.6 and 0.8

Figure 14 Effect of aspect ratio on instability regions of for uniform loaded anti-symmetric angle-ply plate, a/b=1, 2 and 3 $\alpha = 0.2$

Figure 15 Effect of thickness on instability region of a anti-symmetric angle-ply plate a/b=1, α=0.2, a/h=20, 25 and 30

Figure 16 Effect of ply orientation on instability region of a anti-symmetric angle-ply plate for load case 1(a): a)$\alpha = 0.2$, c/b=0.2; b) $\alpha = 0.2$, c/b=0.8.

Figure 17 Effect of ply orientation angle on instability region of a anti-symmetric angle-ply plate for load case 1(b): a) $\alpha = 0.2$, c/b=0.2; b) α=0.2, c/b=0.8.

Figure 18 Effect of ply orientation on instability region of a anti-symmetric angle-ply plate for point loads: a) load case 1(c); b)load case 1(d).